Fibers Based on Cellulose–Silk Fibroin Blend

E. Marsano,[1] M. Canetti,[2] G. Conio,[3] P. Corsini,[1] G. Freddi[4]

[1]*Dipartimento di Chimica e Chimica Industriale, Università di Genova, Via Dodecaneso, 31-16146 Genova, Italy*
[2]*ISMAC-CNR, Sezione di Milano, Via E. Bassini, 15-20133 Milano, Italy*
[3]*ISMAC-CNR, Sezione di Genova, Via De Marini, 6-16149 Genova, Italy*
[4]*Stazione Sperimentale per la Seta, Via G. Colombo, 83-20133 Milano, Italy*

Received 13 December 2004; accepted 27 June 2005
DOI 10.1002/app.24856
Published online in Wiley InterScience (www.interscience.wiley.com).

ABSTRACT: Fibers made of cellulose (CE) and silk fibroin (SF) are wet spun from solutions in *N*,*N*-dimethylacetamide containing 7% LiCl (w/w). Different coagulation baths (water and ethanol) and spinning conditions are used. By using water as the coagulant, a partial dissolution of SF occurs and negligible variation of the mechanical properties of the CE–SF fibers with respect to the CE fibers is found. Fibers coagulated in ethanol are dimensionally homogeneous and show better properties. A modulus of about 13 GPa and elongation to break of 16% for the blend containing 30% (w/w) SF are obtained with a 20-mm air gap. The fibers are characterized by FTIR micro-Raman, scanning electron microscopy, and wide- and small-angle X-ray analyses. In particular, the X-ray results show that CE–SF fibers are amorphous with a homogeneous dispersion of small SF domains (1.3 nm) in the CE matrix. These results confirm the good compatibility between the two natural polymers. © 2007 Wiley Periodicals, Inc. J Appl Polym Sci 104: 2187–2196, 2007

Key words: biopolymers; blends; fibers; cellulose; silk

INTRODUCTION

Cellulose (CE) and silk fibroin (SF) are two natural, biorenewable, and biodegradable polymers that are widely used in the textile industry. Fibroin is a fibrous protein consisting of glycine, alanine, and serine as the main amino acid residues. It is one of the most extensively studied materials. The traditional method to obtain silk involves the meticulous unraveling of fibers from silkworm cocoons and weaving them into fabrics. However, several recent studies are reported on silk fibers produced by spiders, especially the dragline silk from *Nephila clavipes*. The properties of these fibers such as the strength and toughness are better than those of traditional silk from the *Bombyx mori* silkworm and comparable to synthetic high performance fibers.[1–4] Unfortunately, obtaining the silk from the spider is a difficult and time-consuming process. These small creatures are only capable of producing about 1 mg of dragline silk per day.

Other sources of silk fibers are now available. For example, Nexia Biotechnologies based in Montreal has developed transgenic goats that express spider silk proteins in their milk.[1] These proteins have been processed into fibers with the registered trade name BioSteel. Shao and Vollrath[5] have shown that, by changing the reeling conditions and controlling the elongational stress, silkworm silks can be made stronger, stiffer, and more extensible, approaching spider dragline silk properties. This forms the basis for a renaissance in silk materials.

CE is a natural polymer that is a linear (1 → 4) linked β-D-glucopyranose. It is extremely abundant and inexpensive and is widely used in the textile field as cotton, hemp, and jute thanks to its superior moisture absorbing property and biodegradability. CE fibers are also produced as regenerated fibers, such as rayon and polynosic fibers, which are composed of CE-like natural fibers and obtained by a wet spinning process of CE–solvent solutions. However, regenerated CE fiber, in particular rayon, has the defects of poor stiffness and resilience, although they are superior in soft handling and draping.

The chemical composition and molecular conformation of CE allow some peculiar properties to be achieved: the rich hydroxyl groups in CE repetition units promote intramolecular hydrogen bonds that stiffen the chain and simultaneously facilitate the formation of intermolecular hydrogen bonding with other polymers, leading to good miscibility and novel functions and properties.

An interesting peculiarity of CE regarding its chain semirigidity is the capacity to assume liquid crystalline organization in solution. This behavior was exploited to produce high performance fibers by wet spinning of concentrated solutions in various solvents such as *N*,*N*-dimethylacetamide (DMAc),[6] *N*-methyl-morpholine-oxide,[7] and ammonia/ammonium thiocyanate.[8]

Correspondence to: E. Marsano (marsano@unige.it).
Contract grant sponsor: Fondazione Cariplo.

Thus, because CE can evidence liquid crystalline organization in solution, natural silk secretions from ampullae of spiders and silk glands of silkworms form liquid crystalline phases as well.[9] Moreover, it is feasible for silk solutions to exhibit nematic liquid crystallinity via supramolecular assembly of mesogens.[10]

In recent years an increasing interest has been developing for new materials with tailored technological properties combined with favorable environmental impact. The use of biodegradable and environment friendly natural fibers has been a natural choice for filling polymers to make them ''greener,'' for example, CE fibers can be used instead of glass fibers to realize polymeric composites.[11] The reuse of organic wastes, rich in natural polymers, is particularly interesting to attain new regenerated fibers: CE fiber can be obtained from direct spinning of lignocellulosic or wheat straw raw materials.[12,13]

Accordingly, recycling silk wastes, which are short fibers that are not suitable for conventional textile use, may be included in new processes for regenerated fibers. This could represent a challenge for the exploitation of natural renewable resources for manufacturing natural polymers.

The possibility of obtaining homogeneous blends between these natural polymers is a handy and important way to exploit for realizing new environmentally friendly artificial materials. The production of new biofibers using wet spinning processes is also an interesting aspect, considering the strong fibrogenic nature of CE and fibroin.

Studies are reported regarding the phase behavior of blends obtained from regenerated CE with natural or synthetic polymers: CE acetate,[14] chitin,[15] polyacrylonitrile.[16–18] For some samples an improvement of the mechanical properties by blending CE with another natural polymer such as casein[19,20] or alginate[21] is also reported. The blending of fibroin with other polymers is expected to be a useful method to improve its mechanical properties or to develop new functions. Examples of fibroin blends with other polymers include poly(vinyl alcohol),[22,23] chitosan,[24] sodium polyglutamate,[25] and sodium alginate.[26]

Biofibers obtained from wet spinning of blends based on natural polymers are documented for CE–chitin[27–29] (commercialized as Crabyon[30]), CE–SF,[31] SF–chitin,[32] chitosan–SF,[33] and chitosan–tropocollagen fibers.[34]

The present study aims to prepare a new blend of artificial biofibers of CE–SF. It was shown recently that the addition of CE to fibroin was effective in improving the mechanical properties of the blend film obtained by casting in methanol the polymers dissolved in cuoxan, and these properties varied with the blend composition.[31]

In the present work we used DMAc/LiCl as a solvent to dissolve both fibroin and CE and to prepare biofibers from wet spinning of polymer solutions. The effects of different coagulants and spinning conditions on the structure and mechanical properties of the biofibers were investigated and discussed.

EXPERIMENTAL

Materials

An SF sample having a volume-viscosity molecular weight (M_v) of 127,000 was supplied by Stazione Sperimentale per la Seta (Milano, Italy). The SF was a by-product of the ''spun silk'' processing cycle characterized by a very short fiber length, which is unsuitable for any conventional spinning process. The fibrous material contained variable amounts of pupae residues that required a preliminary cleaning procedure. For this purpose the SF was first purified by dissolution in a saturated solution of LiBr (9–10*M*) at 60°C for almost 3 h, followed by filtration (to remove insoluble foreign matters), dialysis, and freeze-drying. The resulting pure SF was obtained in the form of a porous, spongelike material and used for the dissolution tests.

A regenerated CE II (CE) sample with a M_v of 63,000 (degree of polymerization = 390) was supplied by Lenzing AG. CE was purified by treatment with deionized water, acetone, and petroleum ether. Then, it was dried in a vacuum oven at 40°C and maintained under dry conditions. SF and CE samples were used for spinning experiments of neat CE and blends of CE and silk (CE/SF).

DMAc (Fluka) was distilled under a vacuum before use and stored over Riedel type 4-Å molecular sieves. LiCl was dried at 200°C.

Dope preparation

Freeze-dried SF was directly dissolved in DMAc/7% LiCl by heating at 80°C for about 45 min to obtain complete dissolution. Different polymeric concentrations, expressed in weight ratios, were considered. The degradation of the protein chains was determined by viscometry at 25°C in LiBr. The intrinsic viscosity of SF was determined by means of the SNV 195595 standard method. SF was dissolved in a saturated LiBr aqueous solution (9–10*M*) at 60°C for 3 h. After dilution with water (1 : 1, v/v), the viscosity was measured at 20°C with a capillary viscometer. The Mark–Houwink constants were $a = 0.95$ and $K = 2.95 \times 10^{-3}$.[35]

CE was dissolved following a modified method proposed by Turbak et al.,[36,37] obtaining solutions with different weight concentrations (C_p) in DMAc/7% LiCl (w/w). The temperature used for the activation of CE was 140°C instead of 160°C, and the CE

dissolution was verified for samples with molecular weights lower than about 100,000. No polymer degradation was observed. The degree of CE polymerization was estimated by measuring the viscosity; samples were dissolved in cuproethylendiamine (CED) solution (0.5*M*) at 25°C. The viscosity of the solutions was measured with a capillary viscometer at 25°C. The Mark–Houwink constants for CE/CED were $a = 0.905$ and $K = 1.33 \times 10^{-4}$.[38]

Polymer blend solutions were prepared by mixing the two stock solutions or dissolving SF directly in the CE solution, according to the selected polymer composition, which was 70/30 (w/w) CE/SF. The systems were left under stirring for at least 4 days.

Spinning

A wet spinning line, with a 100 micron spinneret die, was used to produce the fibers. The extrusion speed (V_0) was fixed at 7.9 m/min, corresponding to a shear rate at the spinneret of 10,500 s^{-1}. The monofilament was extruded in a coagulation bath at 25°C and collected by a set of spools at a take-up speed (V_1); the filament was finally wound up with a spoon, operated at roller speed (V_r). Fibers were collected using ìas-spunî conditions (no stretch applied during coagulation, $V_1/V_f = 1$) and under a stretching ratio (V_1/V_f) >1, where V_f is the fiber velocity at the spinneret hole; moreover, the roller and take-up speeds were equal ($V_1 = V_r$). When possible, the V_1/V_f was raised to 3. The liquid media used to coagulate both natural polymers were chosen between the most friendly and common nonsolvents for CE and SF (water and ethanol), both at room temperature. The fibers were further washed in the solvent in which they were coagulated (water or ethanol) for about 3–4 days to extract all LiCl salt.

Fiber characterization

Scanning electron microscopy (SEM)

Fiber characterization was performed by using a scanning electron microscope (Cambrige Stereoscan model 440 at 20-kV acceleration voltage) to observe the morphological features of the intact fiber lateral surface. Then, after cryogenically breaking the fiber, the microscope was used to observe the fractured surface.

Optical microscopy

The fiber diameters were determined using an optical microscope. The average diameter was the result of at least 80 measurements and data set distribution was compared with theoretical Gaussian function.

Mechanical properties

The mechanical properties of single fibers were measured using an Instron dynamometer model 5500, with a 50 mm gauge length at a crossbar rate of 5 mm/min, corresponding to strain rate of 1.7×10^{-3} s^{-1}. The elastic modulus (E), breaking strength (σ_b), elongation to break (ε_b), and yield stress (σ_p) at 0.2% were calculated as the average of at least 15 measurements from stress–strain curves.

Raman analysis

Raman spectra were collected with a Renishaw 2000 spectrograph equipped with a liquid nitrogen cooled CCD detector. A diode laser tuned to 785 nm was used for sample excitation. An optical microscope with 50 power objective magnification was utilized to focus the laser beam on the fibers. Forty-nine scans were averaged to achieve an adequate signal to noise ratio from 1800 to 100 cm^{-1}. Raman spectra can be used to obtain information about the secondary structures of proteins and to evaluate the actual amount of CE and SF present in the spun fibers.

For this last purpose films were prepared at different compositions of CE and silk via the solution casting technique using DMAc/LiCl as a common solvent and ethanol as a coagulant solvent. The films and fibers were analyzed at different points to verified the homogeneity of the signal along the samples. A calibration curve, which reports the SF amount as a function of an intensity factor, for the determination of the amount of SF in the film and fibers was developed using the spectral bands of silk amide *I* at 1655 cm^{-1} and CE at 1088 cm^{-1}. An intensity factor (I_r) was created from the peak areas of silk amide *I* (I_{SF}) and CE (I_{CE}) bands according to the following equation:

$$I_r = \frac{I_{SF}}{I_{SF} + I_{CE}}$$

X-ray data

Wide-angle X-ray diffraction (WAXD) data were obtained at 20°C using a Siemens D-500 diffractometer equipped with a Siemens FK 60-10 2000-W tube (Cu Kα radiation, $\lambda = 0.154$ nm). The operating voltage and current were 40 kV and 40 mA, respectively. The data were collected from 5 to 35 2° at 0.02 2° intervals. The fibers were cut, mixed, and pressed to obtain a random panel to submit for the X-ray measurements.

Small-angle X-ray scattering (SAXS) measurements were conducted at 20°C with a Kratky Compact Camera. Monochromatized Cu Kα radiation was supplied by a stabilized Siemens Krystalloflex 710 generator and a Siemens FK 60-04 1500-W Cu target

TABLE I
Intrinsic Viscosity [η] of SF and CE and Corresponding M_v

Sample	[η] (dL/g)	M_v (kDa)
Fibroin fiber	0.294[a]	127
Freeze dried fibroin	0.253[a]	108
Regenerated fibroin[b]	0.228[a]	97
Cellulose	2.15[c]	63
Regenerated cellulose[b]	2.14[c]	63

[a] In LiBr, 9*M*, $T = 25°C$.
[b] Regenerated from DMAc/LiCl solution.
[c] In CED, 0.5*M*, $T = 25°C$.

tube operated at 40 kV and 25 mA. The scattered intensity was counted at 203 angles of measurement in the range from 0.1 to 3.0 2° by using a step scanning proportional counter with pulse height discrimination. Measurements were conducted while orienting the sample fiber axis alternatively in the perpendicular and parallel directions to the primary beam axis. Blank scattering was subtracted from sample scattering after correction for sample absorption. A desmearing data procedure was applied to correct the collimation effects.[39] For all SAXS measurements the abscissa variable was a scattering vector (h), which can be defined as $h = 4\pi \sin\theta/\lambda$.

RESULTS AND DISCUSSION

A new solvent, DMAc/7% LiCl (w/w), was used to dissolve SF and the stability of the solutions was verified. They appeared to be clear and homogeneous and no phase separation was observed. The occurrence of protein degradation was analyzed by viscometric measurements. Table I lists the values of [η] and the corresponding molecular weight (M_v) of SF samples. The first step of dissolution in saturated LiBr solution caused the extent of protein chains degradation to be higher than the subsequent DMAc/LiCl dissolution.

CE solutions, which are easily prepared following the details of the modified Turbak et al. method,[36,37] were clear, homogeneous, and stable. No degradation was found in CE samples dissolved in DMAc/LiCl solution (Table I).

The CE and SF dope concentration, CE/SF ratio, and spinning conditions are key parameters that need optimization before fiber spinning. Although solutions of CE could be easily spun to a concentration over 12% (w/w), SF solutions displayed very low viscosity. The highest SF concentration attained in DMAc–LiCl under the experimental conditions used in this study was 9% (w/w) and its viscosity was so low that it could not be spun. After some attempts, CE and SF blend solutions with a CE/SF weight ratio of 70/30 and different overall C_p values in the range of 5–9% were selected; they were spinnable and no phase separation was observed.

The fibers were produced by using the wet spinning line described in the Experimental section. During the first set of experiments they were collected in a water coagulation bath. Regenerated CE and CE/SF blend fibers were tested for their cross-sectional dimensional and tensile properties. Table II lists the diameters and standard deviations of the fibers coagulated in water. Observe that the diameters decreased as the draw ratio increased and the values were not influenced by the dope polymer concentration. CE/SF blend fibers regenerated in water showed diameter values smaller than the regenerated CE fibers, with larger standard deviations, which was indicative of larger statistical distributions, far from a Gaussian function. This probability function of the normal distribution was calculated theoretically with a normalizing parameter and mean square deviation. The larger statistical distri-

TABLE II
Mechanical Properties of CE and CE/SF Blend Fibers Coagulated in Water

Sample	Silk (%, w/w)	C_p (w/w)	V_1/V_f	Diameter (μm)	E (GPa)	σ_b (MPa)	ε_b (%)	σ_p (MPa)
1a	0	5	1.0	36.0 ± 1.1	14.0 ± 1.6	228 ± 61	13.7 ± 2.8	136 ± 23
1b	0	5	2.0	22.1 ± 1.1	16.3 ± 1.8	249 ± 39	10.2 ± 2.6	139 ± 28
1c	0	5	3.0	20.4 ± 0.8	16.7 ± 0.9	232 ± 47	7.6 ± 2.5	160 ± 17
2a	30	5	1.0	30.0 ± 1.7	16.5 ± 1.7	237 ± 61	6.5 ± 1.5	148 ± 28
2b	30	5	2.0	20.8 ± 1.3	16.4 ± 1.5	160 ± 28	3.4 ± 1.5	143 ± 20
2c	30	5	2.8	18.3 ± 1.0	13.0 ± 2.3	141 ± 30	5.6 ± 4.0	124 ± 58
3a	0	7	1.0	36.0 ± 1.1	15.9 ± 0.6	217 ± 30	13.7 ± 2.6	122 ± 8
3b	0	7	2.0	22.1 ± 0.9	16.8 ± 1.2	218 ± 17	8.3 ± 1.9	133 ± 11
4a	30	7	1.0	30.0 ± 1.7	15.0 ± 0.8	238 ± 5	12.6 ± 1.5	129 ± 6
4b	30	7	2.0	21.6 ± 1.3	15.2 ± 0.6	218 ± 3	14.6 ± 1.4	126 ± 7
4c	30	7	2.8	18.3 ± 1.8	15.4 ± 0.8	193 ± 45	11.2 ± 2.1	132 ± 2
6[a]	100	—	—	9.3 ± 0.3	16 ± 1	650 ± 40	8 ± 6	230 ± 10

[a] *Bombyx mori* silkworm silk determined from single brins (individual fibroin filaments following extraction of sericin).[43]

TABLE III
Amount of SF in CE/SF Fibers Coagulated in Water and Ethanol

Sample	Draw ratio	Take-up rate (m/min)	Res. time (s)	SF content (%, w/w)
4a	1	4.2	14	2–3
4b	2	8.4	7	4–5
4c	2.8	11.7	5	9–10
4d	1.0	3.1	19	28–30

bution of CE/SF blend fibers coagulated in water was attributable to the lack of dimensional homogeneity of the cross section of the fibers.

For the CE samples the modulus and breaking strength were consistent with those reported previously,[6] but slight differences were observed in the improvement in fiber properties by increasing the draw ratio (V_1/V_f). These differences were acceptable, taking into account that the two samples had different average degrees of polymerization and probably different molecular weight distributions.

CE–SF fibers presented mechanical properties values similar to those for CE fibers and no improvement was observed by increasing the draw ratio. This anomalous behavior was shown only for CE/SF blend fibers collected after coagulation in a water bath. Although water represented the best coagulant for CE, this friendly and common solvent was not as effective for silk. When blend fibers were spun and coagulated in water, the solvent likely caused a partial extraction of the protein component, which diffused into the coagulation bath.

To confirm the hypothesis of the partial extraction of SF from the blend fibers, the real fiber composition was measured by Raman analysis. Table III shows the behavior of the blend fiber composition, expressed as the intensity ratio of CE and SF Raman marker bands, as a function of the take-up rate and consequently the residence time of the fibers in the coagulation bath. The amount of silk detected in the blend fibers coagulated in water was lower than expected and the amount of protein extraction was larger for fibers collected at a slower take-up rate, which corresponds to a longer amount of time in the coagulation bath.

Unlike CE, SF is a water-soluble polymer, although its aqueous solutions are metastable and easily undergo coagulation and/or precipitation when they are subjected to various kinds of chemical, physical, or mechanical stresses.[40] Regenerated SF films cast from aqueous solution are still water soluble, until suitable crystallization treatments are performed.[41] This behavior was associated with presence of a prevailing amorphous structure of SF chains in the regenerated films. Therefore, it is reasonable to assume that the as-spun SF component contained in the CE/SF dope coming out of the spinneret and entering the water bath was still water soluble.[40,41]

On the basis of this hypothesis, we decided to change from water to ethanol, a well-known and extensively investigated nonsolvent for SF. In fact, various organic solvents, such as alcohols, have the ability to induce coagulation of SF by the dehydration mechanism, which promotes the formation of intermolecular hydrogen bonds.

The morphology of fibers spun by using ethanol as the coagulant were characterized by means of different microscopic techniques. They appeared homogeneous under optical microscopy observation; CE/SF fibers showed a typical birefringent aspect when observed in polarized light, like CE fibers spun under the same conditions.

SEM microphotographs of CE/SF blend fibers are provided in Figure 1. The surface was smooth with a regular cross-section profile, but a fine longitudinal striation was noticed that was due to irregularity of the spinneret hole. The blend fibers appeared homogeneous, no macroscopic phase separation was observed, and the section was circular.

Raman measurements confirmed that ethanol did not cause any protein extraction from the blend fibers. The Raman spectrum obtained for the 70/30 weight ratio CE/SF blend fibers was comparable to the one obtained from the blend film with the same blending ratio, and the value of the intensity ratio between the Raman marker bands for CE and SF was very close to that expected from the calibration curve (sample 4d, Table III).

The Raman spectrum of SF dissolved in DMAc/LiCl and regenerated as a film by coagulation in an ethanol bath (spectrum a, Fig. 2) showed bands at 1658 (amide I), 1264 and 1227 (amide III), 1083 (CC skeletal stretching), 1000 (vibrational modes of the aromatic ring of Phe and Trp), 978 (ρ_{CH3} modes), and 854 and 830 cm^{-1} (CCH bending of the aromatic ring of Tyr).[42] This spectral pattern indicates that SF chain segments could assume a β-sheet type molecular arrangement, probably because of the annealing effect of the solvent during coagulation and drying. However, the β-sheet nuclei appear poorly organized and immersed into a prevalently amorphous matrix, as suggested by the half-height broadening and low wavenumber position of the amide I band. It is worth noting that other dissolution/coagulation systems were more effective in inducing β-sheet crystallization of regenerated SF.[42]

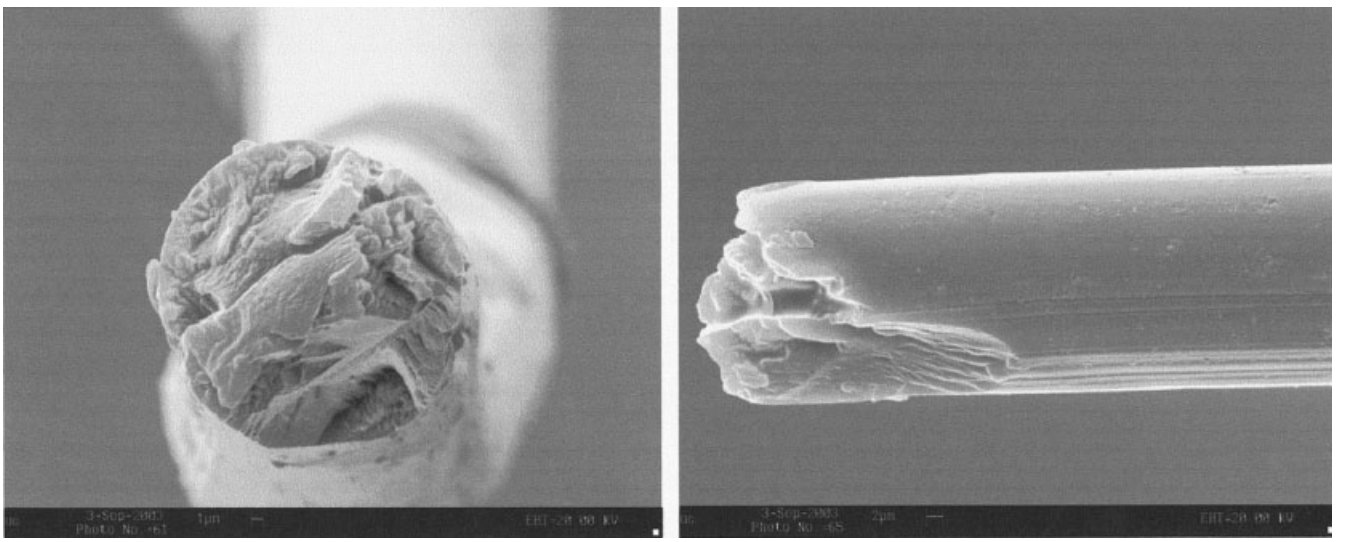

Figure 1 An SEM microphotograph of the CE/SF blend fiber (sample 4e).

Close examination of the Raman spectrum (spectrum b, Fig. 2) of CE/SF blend fibers showed the presence of some of the typical SF bands previously listed, which could be distinguished from those attributable to the cellulosic component. In particular, the amide I at 1658 cm^{-1}, the amide III component at 1227 cm^{-1}, and the two bands at 854 and 830 cm^{-1} are still visible. From their position and intensity it can be inferred that in the blend fiber SF also took a molecular conformation similar to the one in the film. Indeed, SF segments could line up side by side and form short-range β-sheetlike structures. However, they could not grow into well-organized β-sheet crystals, because of the poor annealing effect of the solvent and steric hindrance caused by the presence of large amounts of CE chains.

CE/SF blend fibers regenerated in ethanol showed diameter values similar to those of CE fibers spun at an equal polymer dope concentration ($C_p = 7\%$). The diameters decreased with the draw ratio whereas the tensile properties improved, as can be observed in Table IV. The Young's modulus values were quite similar for CE and CE/SF blend fibers, whereas the latter showed lower σ_b and ε_b values. CE/SF blend fibers exhibited a higher degree of brittleness than CE fibers, which was likely caused by the formation of microvoids during a direct coagulation step in ethanol. This hypothesis could also explain the comparably higher value of the σ_p. The data listed in Table IV do not highlight any differences in the tensile properties as a function of the polymer concentration, although the viscosity of the dope increased with increasing C_p. The higher viscosity of the dope at 9% C_p allowed the application of an air gap ($h = 20$ mm) to the spinning system and to spun CE/SF fibers with improved tensile properties (sample 5c, Table IV). The breaking strength and elongation to break increased significantly, whereas there was no difference in the elastic modulus and yield stress between the fibers spun with or without air gap.

Although the air gap was short, the increased tenacity of the blend fibers could be explained by the formation of a more ordered structure during the passage in air, which prevented the formation of microvoids and microfractures.

Moreover, Table IV provides the mechanical properties of silkworm *B. Mori* Silk fibers.[43] CE–SF fibers have bigger diameters that *B. mori* silk fibers, but the elastic modulus is comparable. The breaking strength and yield stress of regenerated blend fibers are smaller that those of natural silk fibers, which is attributable to the presence of CE in the blend.

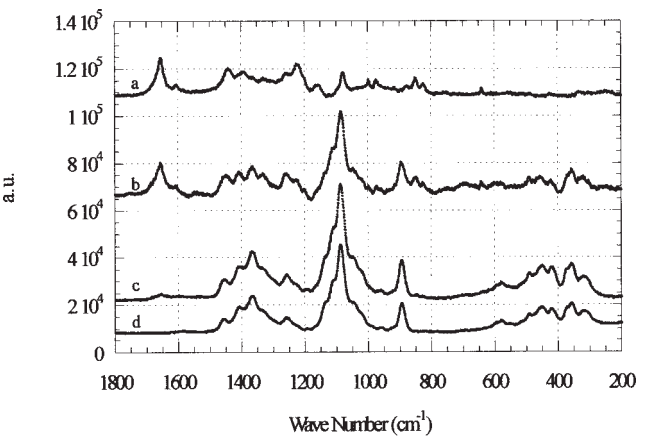

Figure 2 Micro-Raman spectra of an SF film coagulated in ethanol (spectrum a), a CE/SF blend fiber coagulated in ethanol (sample 4e, spectrum b), a CE/SF blend fiber coagulated in water (sample 4b, spectrum c), and a CE fiber (sample 3e, spectrum d).

TABLE IV
Mechanical Properties of CE and SF/CE Blend Fibers Coagulated in Ethanol

Sample	Silk (%, w/w)	C_p (w/w)	V_1/V_f	Diameter (μm)	E (GPa)	σ_b (MPa)	ε_b (%)	σ_p (MPa)
3d	0	7	1.0	36.0 ± 1.1	10.3 ± 1.3	203 ± 7	40.8 ± 6.6	87 ± 12
3e	0	7	2.0	23.3 ± 0.7	16.1 ± 2.4	243 ± 46	13.5 ± 3.6	145 ± 9
3f	0	7	3.0	19.9 ± 0.8	16.3 ± 1.0	252 ± 45	16.4 ± 2.0	143 ± 14
4d	30	7	1.0	36.3 ± 5.5	13.5 ± 1.0	153 ± 25	8.7 ± 3.9	133 ± 14
4e	30	7	2.0	20.9 ± 1.1	16.4 ± 2.1	177 ± 30	2.9 ± 1.1	155 ± 26
5a	30	9	1.0	32.7 ± 3.2	13.3 ± 1.2	163 ± 24	7.8 ± 3.5	130 ± 15
5b	30	9	2.0	26.3 ± 1.0	16.0 ± 0.4	179 ± 29	3.4 ± 1.6	160 ± 6
5c	30	9	1.0	21.6 ± 1.3	12.9 ± 1.6	225 ± 10	15.8 ± 1.8	134 ± 9
6[a]	100	—	—	9.3 ± 0.3	16 ± 1	650 ± 40	8 ± 6	230 ± 10

[a] *Bombyx mori* silkworm silk determined from single brins (individual fibroin filaments following extraction of sericin).[43]

Blend fibers regenerated in ethanol were characterized by means of X-ray techniques. The WAXD profiles of fibers prepared from solutions of pure CE and of CE/SF blends did not show any crystalline evidence, as reported in Figure 3 for samples 4e and 3d. CE precipitated in nonaqueous media can show a very low degree of crystallization.[44]

The difference in the SAXS scattering profile, observed between parallel and perpendicular direction measurements for every sample, was the first evidence of a preferential orientation of the macromolecules in the fibers. However, no meaningful differences were observed in the scattering profiles registered in both directions for CE and blend samples at different draw ratios.

A continuous scattering profile in both directions was registered for the samples prepared using pure CE. The same trend was observed for blend samples analyzed in a perpendicular orientation. Conversely, a discrete region of scattering was observed in the plots relative to blend samples investigated in the parallel direction.

Figure 4 presents the Lorentz-corrected intensity registered in the parallel direction for CE–SF fibers spun with an air gap system. The plot exhibits a maximum relative to a periodicity (L) of the system. The WAXD measurements carried out on all blend samples did not reveal the presence of any crystalline entity. Thus, the periodicity had to be interpreted as the alternation of zones having different electronic

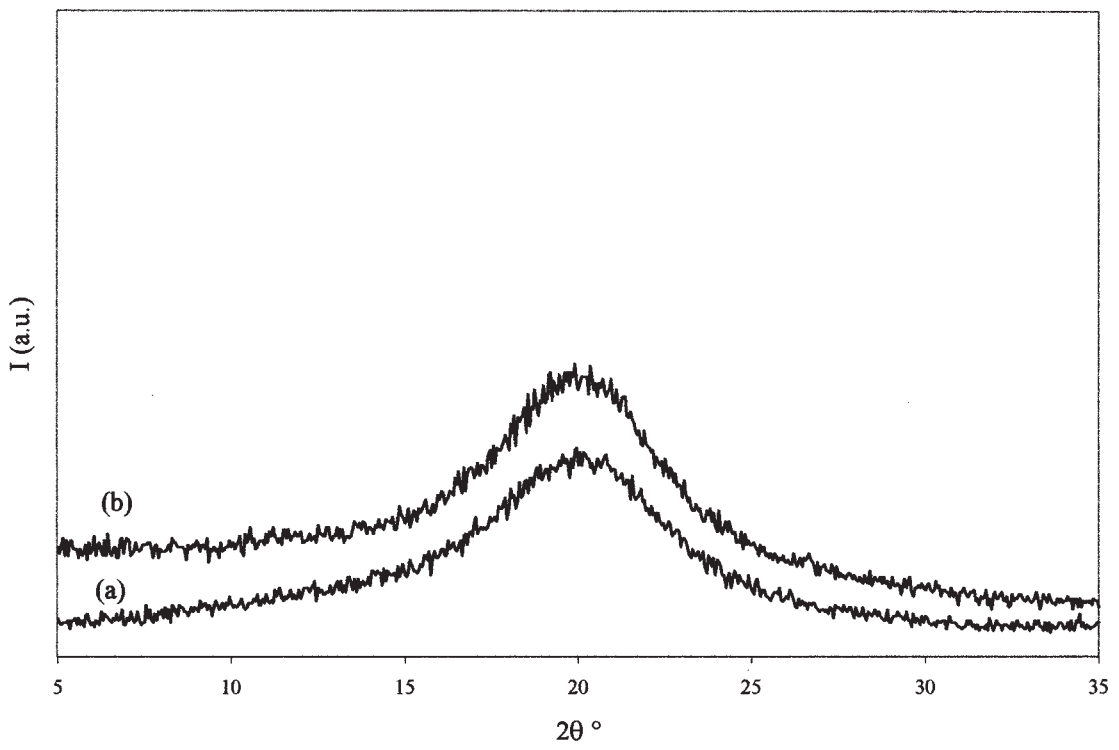

Figure 3 WAXD profiles of (a) CE (sample 3e) and (b) CE/SF blend (sample 4e) fibers.

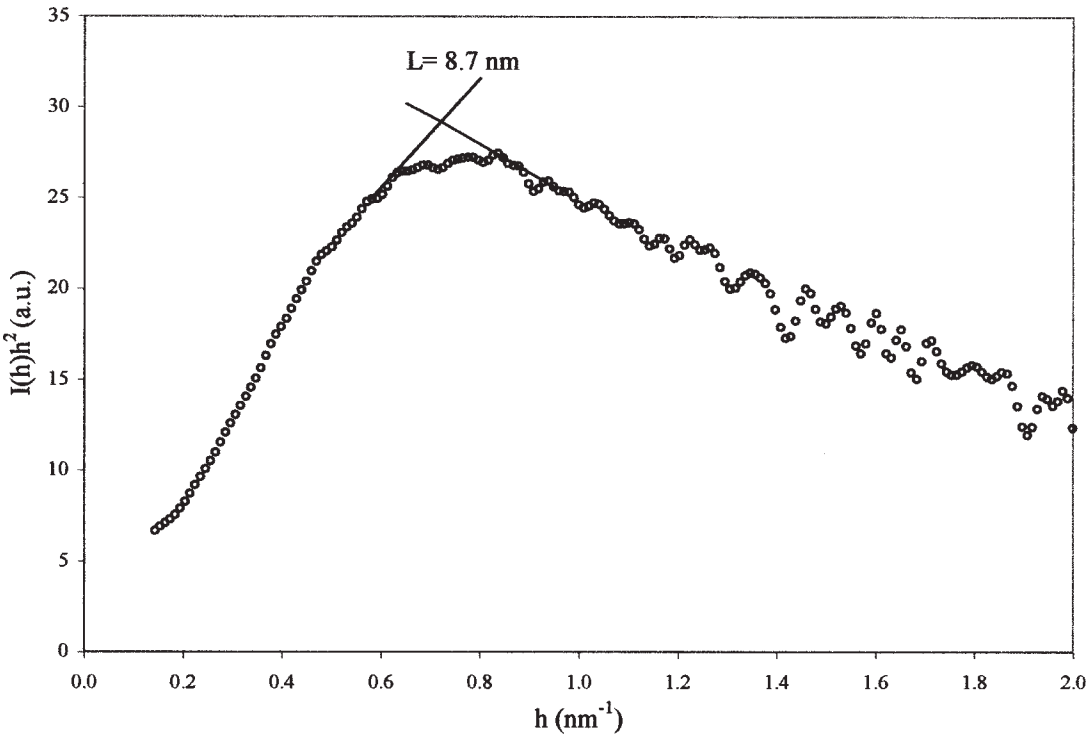

Figure 4 A Lorentz plot of the intensity registered in the parallel direction for a CE/SF fiber (sample 5c).

density, represented by domains of fibroin absorbed in the CE matrix.

A periodicity value between 8.5 and 9.0 nm was extrapolated for some CE–SF fibers (samples 4d, 4e, and 5c, Table IV). The peak broadening observed in all blend samples is an indication of the dispersion of the periodicity dimensional values.

The scattering profile of CE–SF fibers investigated in the parallel direction were analyzed by using the Guinier approximation.[45] Every blend sample showed

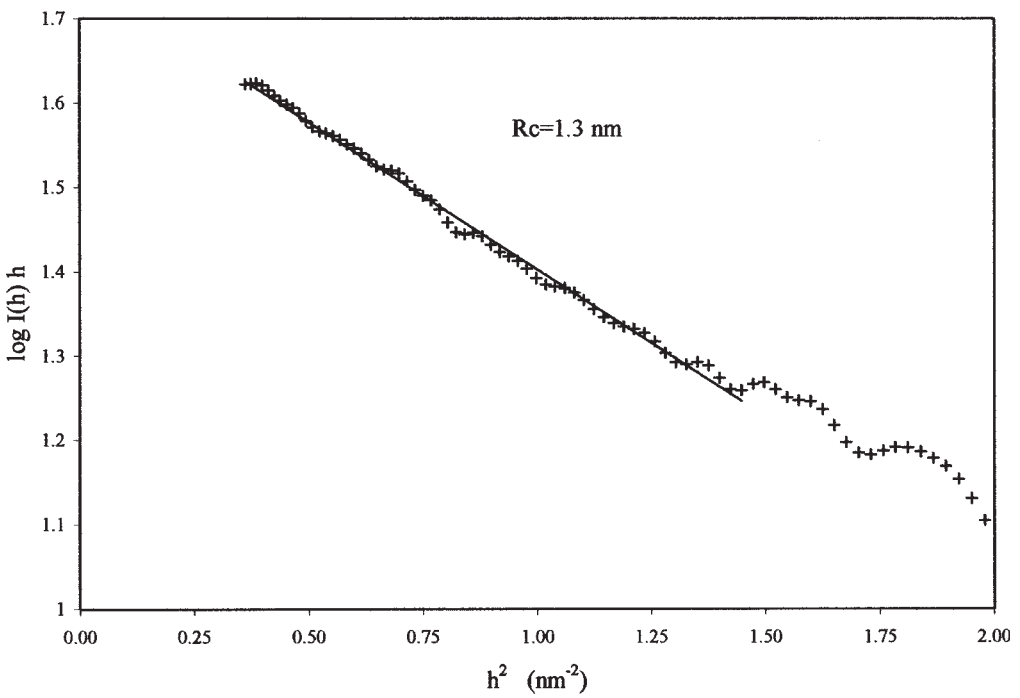

Figure 5 A Guinier plot of the cross section for the CE/SF fiber (sample 5c).

fibroin domains, with parallel dimensions to the fiber axis, which were quite large in comparison to their other lateral dimensions. The sample scattering could be split into two factors; one of them is related to the cross section of the particle in the normal direction to the larger dimension. Multiplying the scattering curve by h, the factor of length could be eliminated and the obtained curves represented only the cross-sectional factor. The radius of gyration of the cross section (R_c) was calculated from the slope of the straight line obtained by plotting log $I(h)h$ versus h^2 for all blend samples.[46] The R_c values of 1.2 $\div$ 1.3 nm were calculated for all investigated CE/SF blend fibers. Figure 5 provides the Guinier plots of sample 5c as an example.

The X-ray results suggest that blends were constituted of domains of fibroin aligned in the fiber direction and dispersed in a CE matrix. For every investigated CE–SF fiber, the SAXS results indicated that fibroin aggregates were able to show periodicity as an indication of regular distribution of domains in the normal direction to the fiber axis.

The continuous scattering profile, which was registered for all samples analyzed in the perpendicular orientation, was an indication of regularity along the fiber direction in terms of electronic density differences.

CONCLUSION

A new method to produce blend fibers of CE and SF was presented. DMAc/LiCl proved to be a good solvent for both natural polymers and it did not cause relevant degradation. CE/SF mixture solutions were homogeneous and stable with time. No phase separations were observed. Moreover, they presented a viscosity that was high enough to be spun with a wet spinning line. The coagulation bath was one of the most important steps in the wet spinning, in particular the nonsolvent used and coagulation time. The residence time of the filament in the coagulation bath composed of water had an effect on the amount of SF in the blend fibers: the longer the time in the bath was, the lower amount of silk. Thus, by changing from water to ethanol, which is a better coagulant for CE–SF fibers, we obtained dimensionally homogeneous fibers with a regular and circular cross section. Moreover, no phase separation was observed in the SEM analysis. Blend fibers with good mechanical properties were observed when an air gap was used.

Furthermore, X-ray analyses showed that CE/SF fibers were essentially amorphous and that there was a homogeneous dispersion of SF domains into the CE matrix.

The cross-sectional size of the SF domain accounted for only a few nanometers, comparable to the dimensions of six to eight protein chains in an ordered conformation. This did not necessarily imply ideal molecular mixing, but it suggested that the level of mixing was adequate to yield the macroscopic properties expected in single-phase materials.

The authors thank the Fondazione Cariplo for financial support through the Fiber on Demand Project and Mr. Mario Traverso for his helpful work on the wet spinning line.

References

1. Lazaris, A.; Arcidiacono, S.; Huang, Y.; Zhou, J. F.; Duguay, F.; Chretien, N.; Welsh, E. A.; Soares, J. W.; Karatzas, C. N. Nature 2002, 295, 472.
2. Vollrath, F.; Knight, D. P. Nature 2001, 410, 541.
3. Kaplan, D. L. Silk Polymers: Materials Science and Biotechnology; ACS Symposium Series 544, ACS: Washington, 1994.
4. Vollrath, F.; Madsen, B.; Shao, Z. Proc R Soc (Lond) 2001, 268, 2339.
5. Shao, Z.; Vollrath, F. Nature 2002, 418, 741.
6. Bianchi, E.; Ciferri, A.; Conio, G.; Tealdi, A. J Polym Sci 1989, 27, 1477.
7. Coulsey, H. A.; Smith, S. B. Lenz Berich 1996, 75, 51.
8. Yang, K. S.; Theil, M. H.; Cuculo, J. A. Polymer Association Structures; ACS Symposium Series 384; American Chemical Society: Washington, DC, 1989.
9. Kerkam, K.; Viney, C.; Kaplan, D. L.; Lombardi, S. Nature 1991, 349, 596.
10. Braun, F. N.; Viney, C. Int J Biol Macromol 2003, 32, 59.
11. Nabi Saheb, D.; Jog, J. P. Adv Polym Technol 1999, 18, 351.
12. Focher, B.; Marzetti, A.; Conio, G.; Marsano, E.; Cosani, A.; Terbojevich, M. J Appl Polym Sci 1994, 51, 583.
13. Marzetti, A.; Focher, B.; Conio, G.; Marsano, E.; Tealdi, A.; Cosani, A.; Terbojevich, M. J Appl Polym Sci 1997, 67, 961.
14. Marsano, E.; Bianchi, E.; Ciferri, A.; Ramis, G.; Tealdi, A. Macromolecules 1986, 19, 626.
15. Bianchi, E.; Marsano, E.; Baldini, M.; Conio, G.; Tealdi, A. Polym Adv Technol 1995, 6, 727.
16. Marsano, E.; Tamagno, M.; Bianchi, E.; Terbojevich, M.; Cosani, A. Polym Adv Technol 1993, 4, 25.
17. Marsano, E.; Conio, G.; Focher, B.; Tamagno, M. Polymer 1994, 35, 168.
18. Marsano, E.; Bianchi, E.; Conio, G.; Tealdi, A. Polym Commun 1994, 35, 3565.
19. Zhang, L.; Yang, G.; Xiao, L. J Membr Sci 1995, 103, 65.
20. Yang, G.; Yamane, C.; Matsui, T.; Miyamoto, L.; Zhang, L.; Okajima, K. Polym J 1997, 29, 316.
21. Zhang, L.; Zhou, D.; Wang, H.; Cheng, S. J Membr Sci 1997, 124, 195.
22. Tanaka, T.; Tanigami, T.; Yamaura, K. Polym Int 1998, 45, 175.
23. Tsukada, M.; Freddi, G.; Crighton, J. S. J Appl Polym Sci 1994, 32, 243.
24. Chen, X.; Li, W.; Zhong, W.; Lu, Y.; Yu, T. J Appl Polym Sci 1997, 65, 2257.
25. Liang, C.; Hirabayashi, K. Sei-I Gakkaishi 1990, 46, 535.
26. Liang, X.; Hirabayashi, K. J Appl Polym Sci 1992, 42, 1937.
27. Hirano, S.; Nakahira, T.; Zhang, M.; Nakagawa, M.; Yoshikawa, M.; Midorikawa, T. Carbohydr Polym 2002, 47, 121.
28. Nogushi, J.; Wada, O.; Seo, H.; Tokura, S.; Nishi, N. Kobunshi Kagaku 1973, 39, 320.
29. Marsano, E.; Conio, G.; Martino, R.; Turturro, T.; Bianchi, E. J Appl Polym Sci 2002, 83, 1825.
30. Yoshikawa, M. Kagaku (Kyoto) 1999, 54, 34.

31. Freddi, G.; Romano, M.; Rosaria, M.; Tsukada, M. J Appl Polym Sci 1995, 56, 1537.
32. Hirano, S.; Nakazawa, M.; Nakahira, T.; Kim, S. K. J Biotechnol 1999, 70, 373.
33. Park, K. H.; Oh, S. Y.; Yoo, D. I.; Shin, Y. Adv Chitin Sci 2000, 4, 122.
34. Hirano, S.; Zhang, M.; Nakagawa, M.; Miyata, T. Biomaterials 2000, 21, 997.
35. Freddi, G.; Berlin, A.; Tsukada, M.; Bubini Paglia, E. Sericologia 2000, 40, 363.
36. Turbak, A.; El-Kafrawy, A.; Snyder, F. W.; Auerbach, A. B. Brit. Pat. Applic. 2,005, 107A (1981).
37. Turbak, A.; El-Kafrawy, A.; Snyder, F. W.; Auerbach, A. B. U.S. Pat. 4,202,25A (1982).
38. Immergut, E. H.; Randy, B.; Mark, E. H. Ind Ing Chem 1953, 45, 2483.
39. Glatter, O.; Gruber, K. J Appl Crystallogr 1993, 26, 512.
40. Magoshi, J.; Magoshi, Y.; Nakamura, S. J. J Polym Sci: Appl Polym Symp 1985, 41, 187.
41. Tsukada, M.; Gotoh, Y.; Nagura, M.; Minoura, N.; Kasai, N.; Freddi, G. J Appl Polym Sci 1994, 32, 961.
42. Monti, P.; Freddi, G.; Bertoluzza, A.; Kasai, N.; Tsukada, M. J Raman Spectrosc 1998, 29, 297.
43. Perez-Rigueiro, J.; Viney, C.; Llorca, J.; Elices, M. J Appl Polym Sci 2000, 75, 1270.
44. Bikales, N. M.; Segal, L. Cellulose and Cellulose Derivatives; Wiley: New York, 1971.
45. Guinier, A.; Fournet, G. Small Angle Scattering of X-Rays; Wiley: New York, 1955.
46. Glatter, O.; Kratky, O. Small Angle X-ray Scattering; Academic: London, 1982.